Proceedings of the
44th IEEE Conference on Decision and Control, and
the European Control Conference 2005
Seville, Spain, December 12-15, 2005

Geometric Observers for Dynamically Evolving Curves

Marc Niethammer, Patricio A. Vela and Allen Tannenbaum

Abstract— **This paper proposes a deterministic observer framework for visual tracking based on non-parametric implicit (level-set) curve descriptions. The observer is continuous-discrete, with continuous-time system dynamics and discrete-time measurements. Its state-space consists of an estimated curve position augmented by additional states (e.g., velocities) associated with every point on the estimated curve. Multiple simulation models are proposed for state prediction. Measurements are performed through standard static segmentation algorithms and optical-flow computations. Special emphasis is given to the geometric formulation of the overall dynamical system. The discrete-time measurements lead to the problem of geometric curve interpolation and the discrete-time filtering of quantities propagated along with the estimated curve. Interpolation and filtering are intimately linked to the correspondence problem between curves. Correspondences are established by a Laplace-equation approach. The proposed scheme is implemented completely implicitly (by Eulerian numerical solutions of transport equations) and thus naturally allows for topological changes and subpixel accuracy on the computational grid.**

I. INTRODUCTION

Following the position of moving objects based on the information delivered by one or multiple optical sensors (e.g., video cameras) is the objective of visual tracking. The need for visual tracking is ubiquitous and a multitude of approaches exist for the solution of this tracking problem. Increasingly, computer vision algorithms are required to provide additional information beyond a simple track point, and more complex algorithms are required to produce the desired information. For noisy, cluttered, and/or dynamic scenes the ability of these algorithms to provide a smooth and faithful signal may be questionable. The ability to filter the signals coming from computer vision algorithms will be essential in such scenarios.

This paper considers the observation problem where object position and additional state information needs to be inferred from discrete-time image measurements. Observer design requires a dynamical model of the system to be observed and measurements that will make the observer (as a dynamical system) stable and robust with respect to unknown disturbances (e.g., measurement and system noise) and – especially in the context of visual tracking – with respect to unmodeled dynamics.

The type of observer used for a specific visual tracking problem is directly related to the geometric and dynamic description chosen for the object(s) to be tracked, some of which lead to descriptions by means of coupled ordinary differential equations (in the finite-dimensional case), or coupled partial differential equations (in the infinite-dimensional case). This paper develops a geometric observer framework for *dynamically evolving curves*. It is closest in spirit to previous work on joint segmentation and registration by Yezzi and Soatto [1] and the resulting tracking methodology [2]. While Yezzi and Soatto [1] and Jackson [2] propose a finite dimensional motion model with an overlayed deformation to account for deviations from a current shape template, this paper proposes the use of an infinite dimensional motion model whose motion gets implicitly constrained by the measurement (which itself can be unconstrained, shape-constrained, area-based, etc.). The chosen motion model allows for the tracking of objects with changing topology; a global motion model describing the arbitrary splitting or merging of an object is not required.

Endowing every curve point with additional state information, requires a correspondence scheme between the measured and estimated curves. For the purpose of this paper it is crucial to establish one-to-one correspondences between the measured and the estimated curves in order to determine unique "distances" between points and to exchange information between them for dynamic filtering. The distance-measurements allow for a geometric interpolation between measurement and estimated curve, facilitating geometric, intuitively tunable gains for position filtering. The observer structure is flexible enough to entertain the case where filtering position information is not utilized and may be replaced by static position measurements in case of clearly segmentable image data, leading to reduced order observers whose associated state information still needs to be filtered.

For presentational simplicity, this paper is restricted to dynamically evolving curves (see Section II). However, the overall scheme extends to closed hypersurfaces of codimension one. Section II briefly reviews curve evolution equations, related notation, and level set implementations. Section III introduces the general observer structure used in this paper. Section IV describes different possible motion models (priors) for the observer. Measurements are covered in Section V. Section VI explains the error correction scheme. Reduced order observers are introduced in Section VII. Results are presented in Section VIII. Conclusions are given and future work is discussed in Section IX.

II. CURVE EVOLUTION

A planar curve evolution may be described as the time-dependent mapping: $\mathcal{C}(p,t) : S^1 \times [0,\tau) \mapsto \mathbb{R}^2$, where $p \in [0,1]$ is the curve's parameterization on the unit circle S^1,

This work was supported in part by grants from AFOSR, ARO, NSF, NIH (through NAC Brigham and Women's Hospital), MRI-HEL, and MURI.

Marc Niethammer, Patricio A. Vela, and Allen Tannenbaum are with the School of Electrical and Computer Engineering, Georgia Institute of Technology, Atlanta, GA 30332-0250, {marcn,pvela,tannenba}@ece.gatech.edu.

0-7803-9568-9/05/$20.00 ©2005 IEEE

$\mathcal{C}(p,t) = [x(p,t),\ y(p,t)]^T$, and $\mathcal{C}(0,t) = \mathcal{C}(1,t)$. Define the interior and the exterior of a curve $\mathcal{C}$ on the domain $\Omega \subset \mathbb{R}^2$ as

$$\begin{aligned} int(\mathcal{C}) &:= \left\{ \boldsymbol{x} \in \Omega : (\boldsymbol{x} - \boldsymbol{x}_c)^T \mathcal{N} > 0,\ \forall \boldsymbol{x}_c \in \mathcal{C} \right\}, \\ ext(\mathcal{C}) &:= \Omega \setminus \overline{int(\mathcal{C})}, \end{aligned}$$

where $\mathcal{N}$ is the unit inward normal to $\mathcal{C}$. To avoid tracing individual curve particles over time $\mathcal{C}$ can be represented implicitly by a level set function $\Psi : \mathbb{R}^2 \times [0,\tau) \to \mathbb{R}$ [3], where

$$\Psi(0,t)^{-1} = trace(\mathcal{C}(\cdot,t)).$$

There is no unique level set function Ψ for a given curve $\mathcal{C}$. Frequently, Ψ is chosen to be a signed distance function, defined as follows:

$$\begin{cases} \|\nabla\Psi\| = 1, \text{ almost everywhere}, \\ \Psi(\boldsymbol{x}) = 0,\ \forall \boldsymbol{x} \in \mathcal{C}, \\ \Psi(\boldsymbol{x}) < 0,\ \forall \boldsymbol{x} \in int(\mathcal{C}), \\ \Psi(\boldsymbol{x}) > 0,\ \forall \boldsymbol{x} \in ext(\mathcal{C}). \end{cases}$$

Given a curve evolution equation

$$\mathcal{C}_t = \boldsymbol{v},$$

where $\boldsymbol{v}$ is a velocity vector, the corresponding level set evolution equation is

$$\Psi_t + \boldsymbol{v}^T \nabla\Psi = 0.$$

The unit inward normal, $\mathcal{N}$, and the signed curvature, κ, are given by

$$\mathcal{N} = -\frac{\nabla\Psi}{\|\nabla\Psi\|}, \quad \kappa = \nabla \cdot \frac{\nabla\Psi}{\|\nabla\Psi\|}.$$

III. GENERAL OBSERVER STRUCTURE

Assume that the system to be observed evolves in continuous time and that measurements of the system's states become available at discrete time instants $k \in \mathbb{N}_0^+$, i.e.,

$$\begin{aligned} \begin{pmatrix} \mathcal{C} \\ \boldsymbol{q} \end{pmatrix}_t &= \begin{pmatrix} \boldsymbol{v}(\mathcal{C}, \boldsymbol{q}, t) \\ \boldsymbol{f}(\mathcal{C}, \boldsymbol{q}, t) \end{pmatrix} + \boldsymbol{w}(t) \\ \boldsymbol{z}_k &= \boldsymbol{h}_k \left(\begin{pmatrix} \mathcal{C} \\ \boldsymbol{q} \end{pmatrix} \right) + \boldsymbol{v}_k = \begin{pmatrix} \mathcal{C}(t_k) \\ \boldsymbol{q}(t_k) \end{pmatrix} + \boldsymbol{s}_k(t), \end{aligned}$$

where $\boldsymbol{w}$ and $\boldsymbol{s}_k$ are the system and measurement noises respectively, $\mathcal{C}$ represents the curve position, and $\boldsymbol{q}$ denotes additional states transported along with $\mathcal{C}$ (e.g., velocities). Assume further there is a simulation and a measurement model of the form

$$\begin{pmatrix} \hat{\mathcal{C}} \\ \hat{\boldsymbol{q}} \end{pmatrix}_t = \begin{pmatrix} \hat{\boldsymbol{v}}(\hat{\mathcal{C}}, \hat{\boldsymbol{q}}, t) \\ \hat{\boldsymbol{f}}(\hat{\mathcal{C}}, \hat{\boldsymbol{q}}, t) \end{pmatrix}, \quad \hat{\boldsymbol{z}}_k = \begin{pmatrix} \hat{\mathcal{C}}(t_k) \\ \hat{\boldsymbol{q}}(t_k) \end{pmatrix},$$

where the hat denotes estimated quantities. Assuming $\boldsymbol{h}_k = id$ (the identity map), corresponds to a completely measurable state $\boldsymbol{x} = [\mathcal{C}, \boldsymbol{q}]^T$. The proposed continuous-discrete observer is formally

$$\begin{aligned} \begin{pmatrix} \hat{\mathcal{C}} \\ \hat{\boldsymbol{q}} \end{pmatrix}_t &= \begin{pmatrix} \hat{\boldsymbol{v}}(\hat{\mathcal{C}}, \hat{\boldsymbol{q}}, t) \\ \hat{\boldsymbol{f}}(\hat{\mathcal{C}}, \hat{\boldsymbol{q}}, t) \end{pmatrix}, \quad \hat{\boldsymbol{z}}_k = \begin{pmatrix} \hat{\mathcal{C}}(t_k) \\ \hat{\boldsymbol{q}}(t_k) \end{pmatrix}, \quad (1) \\ \begin{pmatrix} \hat{\mathcal{C}}_k(+) \\ \hat{\boldsymbol{q}}_k(+) \end{pmatrix} &= \begin{pmatrix} \hat{\mathcal{C}}_k(-) \\ \hat{\boldsymbol{q}}_k(-) \end{pmatrix} +^* \begin{pmatrix} K_k^{\mathcal{C}} *^* \left(\mathcal{C}_k -^* \hat{\mathcal{C}}_k(-) \right) \\ \boldsymbol{K}_k^{\boldsymbol{q}} *^* \left(\boldsymbol{q}_k -^* \hat{\boldsymbol{q}}_k(-) \right) \end{pmatrix}, \end{aligned}$$

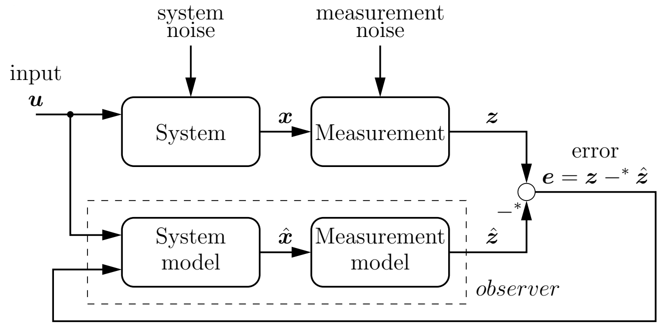

Fig. 1. General Observer Structure. The error e is implicitly defined by means of a correspondence procedure. The measurement makes use of standard segmentation algorithms and the system model is given by a chosen prior.

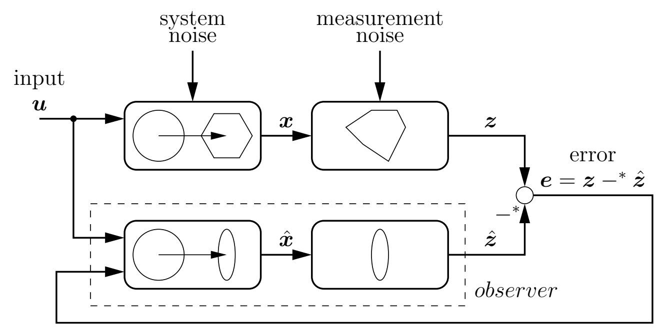

Fig. 2. Symbolic Observer Structure. How does one perform these computations on and with curves?

where $(-)$ denotes the time just before a discrete measurement, $(+)$ the time just after the measurement, and $K_k^{\mathcal{C}}$ (a scalar) and $\boldsymbol{K}_k^{\boldsymbol{q}}$ (a diagonal matrix of scalars) are the decoupled error correction gains for the curve position $\mathcal{C}$ and the additional state quantities $\boldsymbol{q}$ respectively. The operators $-^*$, $+^*$, $*^*$ denote subtraction, addition, and multiplication of curves and of the additional state quantities propagated with the curves respectively. They are a crucial part of the proposed observer framework. Figures 1 and 2 show the observer structure as given in Equation (1).

Section IV discusses different system models (priors) to predict the estimated curve's position and the change of additional state quantities over time. Measurements are described in Section V, they consist of a static segmentation at every discrete time instant to measure position and measurements of additional state quantities (e.g., velocities) at this measured location. The measurement model is the identity map (see Equation (1)). Finally, the error correction scheme (establishing the combined meaning of the operators $+^*$, $-^*$, and $*^*$) is given in Section VI.

IV. PRIORS

The prediction part is a motion prior. It is problem dependent and should model as precisely as possible the dynamics of the object(s) to be tracked. Ideally the measurement part of an observer should only need to correct for inaccuracies due to noise. However, in practice it will be difficult (or even impossible) to provide an exact motion model so that the measurement part also needs to compensate for inaccuracies of the motion prior.

The following sections propose three increasingly complex priors: the static prior, the quasi-dynamic optical flow prior, and the dynamic elastic prior. These should be pointers to relatively general-purpose priors. They should be substituted by more accurate (problem-specific) priors if available. For now only curve evolutions with velocities normal to the curve are allowed.

A. Static Prior

The simplest possible prior is the static prior, i.e., the motion model assumes no motion at all.

$$\hat{\mathcal{C}}_t = \mathbf{0}.$$

For visual tracking the movement of a curve is then only driven by the measurement part of the observer. Were it not for the measurements, the curve would stay fixed at one position.

B. Quasi-dynamic Optical Flow Prior

The quasi-dynamic optical flow prior uses optical flow information as a motion prior, i.e., the simulation part of a normally evolving curve would be given by

$$\hat{\mathcal{C}}_t = (\boldsymbol{v}_{OF} \cdot \mathcal{N})\mathcal{N},$$

where $\boldsymbol{v}_{OF}$ is the measured optical flow velocity (see Section V-B for details on optical flow computations)[1].

C. Dynamic Elastic Prior

The dynamic elastic prior is based on the dynamic active contour [4], where the action integral

$$\mathcal{L} = \int_{t=t_0}^{t_1} \int_0^1 \left(\frac{1}{2}\mu \|\hat{\mathcal{C}}_t\|^2 - a \right) \|\hat{\mathcal{C}}_p\| dp dt \qquad (2)$$

is minimized. In Equation (2) μ denotes a mass constant and a a scalar regularization field. Whereas a is image-dependent in the case of a dynamic active contour, it is image-*independent* for the dynamic elastic prior; a is a design parameter for curve regularization (it can either be a constant or a function over space and time). Priors should not depend on underlying image (measurement) information.

The dynamic elastic prior is then given by (see [4] for a derivation)

$$\begin{aligned}\mu\hat{\mathcal{C}}_{tt} = &-\mu(\mathcal{T}\cdot\hat{\mathcal{C}}_{ts})\hat{\mathcal{C}}_t - \mu(\hat{\mathcal{C}}_t\cdot\hat{\mathcal{C}}_{ts})\mathcal{T} \\ &- \left(\frac{1}{2}\mu\|\hat{\mathcal{C}}_t\|^2 - a\right)\kappa\mathcal{N} - (\nabla a\cdot\mathcal{N})\mathcal{N}\end{aligned}$$

or restricted to normal curve propagation by

$$\mu\hat{\mathcal{C}}_{tt} = \left(\frac{1}{2}\mu\|\hat{\mathcal{C}}_t\|^2 + a\right)\kappa\mathcal{N} - (\nabla a\cdot\mathcal{N})\mathcal{N} - \frac{1}{2}\mu(\|\hat{\mathcal{C}}_t\|^2)_s\mathcal{T}. \qquad (3)$$

[1] Technically, this is (in the setting of this paper) not a proper prior, since it implicitly depends on the image through the optical flow calculation.

Here, s denotes arclength and $\mathcal{T}$ is the unit tangent vector to $\hat{\mathcal{C}}$.

D. Other Possibilities for Dynamic Priors

Additional dynamic priors are conceivable. Particularly interesting research directions might be dynamic priors that are area-preserving, length-preserving, smoothness-limiting, etc. Shape-restrictions for dynamic priors could for example be accomplished by projecting the dynamic evolution onto a certain, specified shape equivalence class.

V. MEASUREMENTS

Measurements are used to drive the estimated model's states to the true system states. This is necessary, since generally the system model will be imperfect and the designed observer needs to be robust with respect to disturbances. For visual tracking, it is difficult to come up with accurate motion models, meaning that simple approximations need to suffice.

The simulated measurement is based on the current state of the estimated curve (the current state of the observer), i.e., its current position, velocities, etc. Any of the standard segmentation algorithms can be used to come up with the "real" measurement that the simulated one has to be compared against to define the error measure.

This observer setup has two crucial advantages:

- Any standard (static or dynamic) segmentation algorithm can be employed for the measurement. While the dynamic model is a model of a dynamically evolving curve, the measurement can utilize, for example, area-based or region-based segmentation algorithms.
- Static and dynamic approaches incorporating shape information exist [1], [5]. If these approaches are used for the measurement curve, shape information can be induced into the infinite dimensional model without the need for explicit incorporation of the shape information into the dynamical model.

The incorporation of shape-information as a constraint on the measurements contrasts with previous approaches aimed at including shape information into the dynamics of an evolving curve itself, e.g., the condensation filter based curve trackers of Blake and Isard [6] where motion is restricted to affine motion. Using a finite dimensional motion group reduces the dimensionality of the evolution state space. Whereas a general curve evolution is infinite-dimensional, affine motion constraints lead to finite-dimensional descriptions and are thus relatively easy to implement and usually fast. To account for (in many cases likely) deviations from the motion model, correction terms need to be introduced, as is done in the deformotion work by Yezzi and Soatto [1].

A. Position Measurements

Position measurements can be accomplished by any static segmentation method, which may include shape information. Potential candidates are the classical geodesic active contour

$$\mathcal{C}_t = g\kappa\mathcal{N} - (\nabla g\cdot\mathcal{N})\,\mathcal{N},$$

minimizing

$$\mathcal{L} := \int_0^1 g(\mathcal{C})\|\mathcal{C}_p\|dp,$$

or, for example, active contours without edges [7]

$$\mathcal{C}_t = \left(\mu\kappa - \nu - \lambda_1(u_0 - c_1)^2 + \lambda_2(u_0 - c_2)^2\right)\mathcal{N},$$

minimizing

$$\mathcal{L} := \mu \int_0^1 \|\mathcal{C}_p\|dp + \nu\ area(int(\mathcal{C}))+$$
$$\lambda_1 \int_{int(\mathcal{C})} |u_0(x,y)-c_1|^2 d\Omega + \lambda_2 \int_{\Omega\setminus\overline{int(\mathcal{C})}} |u_0(x,y)-c_2|^2 d\Omega.$$

B. Measurement of Additional Quantities

Measurements of additional state quantities are performed at the location of the position measurements. In case of dynamically evolving curves, velocities need to be measured on the measured curve. Assuming that there is strong edge information at the boundaries of the measured curve, normal optical flow can be computed as

$$\begin{pmatrix} u \\ v \end{pmatrix} = -I_t \frac{\nabla I}{\|\nabla I\|^2},$$

where $I : \mathbb{R}^2 \mapsto \mathbb{R}$ (usually image intensity). If there is no strong boundary information, i.e., when using a position measurement with shape information under partial occlusions of an object to be tracked, regularization has to be performed to obtain the optical flow field reliably; one possibility being the computation of Horn and Schunck optical flow, minimizing

$$\mathcal{L}(I) = \lambda \iint \left(I_x u + I_y v + I_t\right)^2\ dx\ dy$$
$$+ \iint \left(\|\nabla u\|^2 + \|\nabla v\|^2\right)\ dx\ dy.$$

VI. ERROR CORRECTION

The observer framework proposed in this paper requires a methodology to associate an estimated curve state to a measured curve state. This amounts to establishing correspondences between points on the measured and the estimated curve. The correspondence map between measured and estimated curve should be diffeomorphic. Such a diffeomorphic map can be obtained if the estimated and measured curves have the same topology, otherwise the conditions for this mapping between curves need to be relaxed. Section VI-A explains how to establish one-to-one correspondences between curves. Section VI-B discusses the propagation of information along a vector field and the implicit computation of signed distance functions. Curve interpolation is described in Section VI-C. The results of Sections VI-A-VI-C are used in Section VI-D for the error correction scheme.

A. Establishing Correspondences

Inspired by [8], [9], [10] one-to-one correspondences can be established by solving a Laplace equation between the estimated and the measured curves. Given the estimated curve $\hat{\mathcal{C}}$ and the measured curve $\mathcal{C}$ define

$$\begin{aligned} R &:= \overline{int(\hat{\mathcal{C}}) \ominus int(\mathcal{C})}, \\ R_{pi} &:= int(\hat{\mathcal{C}}) \cap int(\mathcal{C}), \\ R_{lo} &:= \Omega \setminus \left(\overline{R \cup R_{pi}}\right). \end{aligned}$$

Compute the solution to

$$\begin{aligned} \Delta u_s(\boldsymbol{x}) &= 0, \quad \boldsymbol{x} \in R \\ \Delta u_{pi}(\boldsymbol{x}) &= c \quad\ \ \boldsymbol{x} \in \overline{R_{pi}},\ c > 0 \\ \Delta u_{lo}(\boldsymbol{x}) &= 0, \quad \boldsymbol{x} \in \overline{R_{lo}}, \end{aligned}$$

with boundary conditions

$$\begin{aligned} u_s(\boldsymbol{x}) &= 0,\ \boldsymbol{x} \in \partial\overline{R_{pi}} \setminus \left(\hat{\mathcal{C}} \cap \mathcal{C}_m\right), \\ u_s(\boldsymbol{x}) &= 1,\ \boldsymbol{x} \in \partial\left(R \cup R_{pi}\right), \\ u_{pi}(\boldsymbol{x}) &= 0,\ \boldsymbol{x} \in \partial\overline{R_{pi}}, \\ u_{lo}(\boldsymbol{x}) &= 1,\ \boldsymbol{x} \in \partial\left(R \cup R_{pi}\right), \\ u_{lo}(\boldsymbol{x}) &= 2,\ \boldsymbol{x} \in \partial\Omega. \end{aligned}$$

The combined solution

$$u(\boldsymbol{x}) = \begin{cases} u_{lo}(\boldsymbol{x}), & \boldsymbol{x} \in R_{lo}, \\ u_{pi}(\boldsymbol{x}), & \boldsymbol{x} \in R_{pi}, \\ u_s(\boldsymbol{x}), & \boldsymbol{x} \in R \end{cases}$$

induces a gradient field $\boldsymbol{v}$

$$\boldsymbol{v}(\boldsymbol{x}) = \begin{cases} \nabla u, & \boldsymbol{x} \in R, \\ \nabla u_o, & \boldsymbol{x} \in R_{lo}, \\ \nabla u_i, & \boldsymbol{x} \in R_{pi} \end{cases}$$

on Ω, which in turn establishes a one-to-one correspondence between points on the curves $\hat{\mathcal{C}}$ and $\mathcal{C}$. Intersection points between $\hat{\mathcal{C}}$ and $\mathcal{C}$ are assumed to correspond to each other. Identifying intersection points as correspondence points is a design choice that removes the need for curve registration, but may lead to perceptually "incorrect" correspondences that the error correction needs to be able to tolerate. Correspondences can be computed as long as

$$int(\hat{\mathcal{C}}) \cap int(\mathcal{C}) \neq \emptyset,$$

otherwise estimate and measurement are in severe disagreement and a loss-of-track procedure needs to be employed (e.g., declaring the measurement as the estimate, or leaving the estimate unchanged, or registering estimate and measurement). Figure 3 illustrates the solution domains.

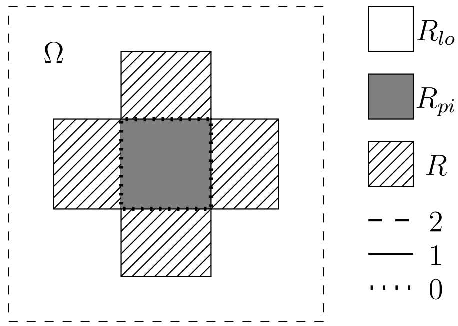

Fig. 3. Solution domains.

B. Transporting Information

Curve evolution is performed implicitly (by means of a level set evolution). Obtaining a completely implicit observer requires implicit information transport between the measured and the estimated curves. Given the advection equation with source term s and velocity field $\boldsymbol{v}$

$$q_t + \boldsymbol{v}^T \nabla q = s \tag{4}$$

the characteristic curves [11]

$$X'(t) = \boldsymbol{v}(X(t))$$

fulfill the ordinary differential equation

$$\frac{d}{dt} q(X(t), t) = s.$$

Thus, to advect vector quantities Ξ along a velocity field $\boldsymbol{v}$, solve

$$\begin{cases} \Xi(\cdot, 0) = \Xi_0, \\ \Xi_t + D\Xi\boldsymbol{v} = \boldsymbol{0}, \end{cases} \tag{5}$$

and to measure traveling distances solve

$$\begin{cases} d = 0, \\ d_t + \frac{\boldsymbol{v}^T}{\|\boldsymbol{v}\|} \nabla d = 1, \end{cases} \tag{6}$$

where $\boldsymbol{v} \neq 0$ is assumed. Equations (4)-(6) are Hamilton-Jacobi equations. Efficient numerical methods exist [12] to compute steady-state solutions of Hamilton-Jacobi equations.

C. Curve Interpolation

An interpolated curve between two curves (in the case of this paper, the estimated and the measured curve) can be obtained by means of a correspondence scheme. If the correspondences are given implicitly through a vector field, geometric interpolation is achieved by measuring the distance between correspondence points (along the characteristic that connects them) and subsequent "marching" up to a certain percentage of this distance. If $\hat{\Psi}$ and Ψ implicitly represent the curves $\hat{\mathcal{C}}$ and $\mathcal{C}$ this interpolation can be accomplished completely implicitly with subpixel accuracy. Solve

$$\begin{aligned} \hat{d}_t + S(\hat{\Psi})\boldsymbol{v}^T \nabla \hat{d} = S(\hat{\Psi}), \quad & \hat{d}(\boldsymbol{x}, 0) = \hat{\Psi}, \\ (d_m)_t + S(\Psi)\boldsymbol{v}^T \nabla d_m = S(\Psi), \quad & d_m(\boldsymbol{x}, 0) = \Psi, \end{aligned} \tag{7}$$

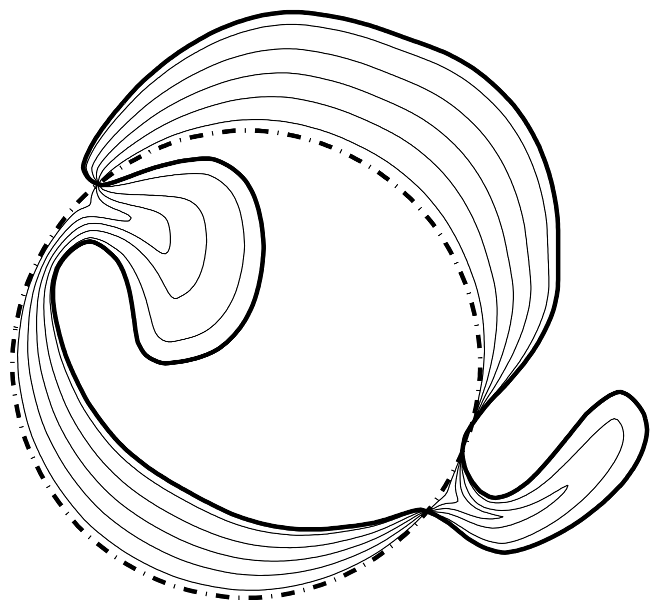

Fig. 4. The solid curve gets geometrically interpolated to the dash-dotted curve.

where

$$S(x) := \begin{cases} 0, & \text{if } \|x\| \leq 1, \\ \frac{x}{\sqrt{\epsilon + x^2}}, & \text{otherwise.} \end{cases}$$

The warped distance functions obtained by solving Equation (7) are interpolated to yield the interpolated warped distance function d_i

$$d_i = (1 - w)\hat{d} + w d_m, \; w \in [0, 1],$$

which subsequently gets redistanced to obtain a new distance function $\hat{\Psi}_i$

$$(\hat{\Psi}_i)_t + S(\hat{\Psi}_i^0)\|\nabla \hat{\Psi}_i\| = S(\hat{\Psi}_i^0), \quad \hat{\Psi}_i(\boldsymbol{x}, 0) = d_i.$$

The weighting factor w geometrically interpolates the estimated and the measured curve. This interpolation is illustrated in Figure 4.

D. Performing the Error Correction

The error correction scheme builds on the results of Sections VI-A-VI-C. Performing error correction for the curve position:

$$\hat{\mathcal{C}}_k(+) = \hat{\mathcal{C}}_k(-) +^* K_k^{\mathcal{C}} *^* \left(\mathcal{C}_k -^* \hat{\mathcal{C}}_k(-) \right)$$

amounts to curve interpolation where

$$trace(\hat{\mathcal{C}}_k(+)) = \hat{\Psi}_i(0)^{-1}, \quad K_k^{\mathcal{C}} = w = w_k.$$

For the error correction of additional state quantities

$$\hat{\boldsymbol{q}}_k(+) = \hat{\boldsymbol{q}}_k(-) +^* \boldsymbol{K}_k^{\boldsymbol{q}} *^* (\boldsymbol{q}_k -^* \hat{\boldsymbol{q}}_k(-)),$$

state information needs to be exchanged and compared between the measured and the estimated curves. The final filtering results needs to be associated with $\hat{\mathcal{C}}_k(+)$. The information exchange is performed by information propagation. For the measured quantities $\boldsymbol{q}_i$

$$(\boldsymbol{p}_i)_t + S(\Psi)\boldsymbol{v}^T\nabla(\boldsymbol{p}_i) = 0, \quad \boldsymbol{p}_i(\boldsymbol{x}, 0) = \boldsymbol{q}_i,$$

and for the estimated quantities $\hat{\boldsymbol{q}}$

$$(\hat{\boldsymbol{p}}_i)_t + S(\hat{\Psi})\boldsymbol{v}^T\nabla\hat{\boldsymbol{p}}_i = 0, \quad \hat{\boldsymbol{p}}_i(\boldsymbol{x}, 0) = \hat{\boldsymbol{q}}_i.$$

Simple (point-wise) filtering results in

$$(\hat{\boldsymbol{q}}_i)_k(+) = (\hat{\boldsymbol{p}}_i)_k + (\boldsymbol{K}_{ii})_k^{\boldsymbol{q}}\left((\boldsymbol{p}_i)_k - (\hat{\boldsymbol{p}}_i)_k\right).$$

VII. REDUCED ORDER OBSERVERS

The described observer thus far was a full order observer, i.e., all system states are observed.

In certain cases it is not desirable to use filtered quantities to observe states. If for example a measurement results in a perfect (or near perfect) measurement of a curve's position, this position information may be used directly (without curve interpolation). Additional state quantities (e.g., velocities) are then dynamically filtered at the measured curve position. Removing the dynamical filtering of states different than the position results in an analogous (reduced) observer structure.

Combining the reduced observer idea with respect to position and the static prior, the position measurement becomes the ground truth. Without additional states to filter such an observer amounts to position tracking based on static segmentations at every image frame, where the initial position condition is the position at the previous time step. Such an observer is identical to static segmentation if the underlying image does not change over time. Thus, the limiting case of a reduced order state observer is static segmentation. The same holds for the quasi-dynamic optical flow prior, however, the initial conditions depend on image information at the current position.

VIII. RESULTS

Figures 5 and 6 show tracking results on a single blob and on two blobs respectively. In both cases the dynamic elastic prior was used with $\mu = 1$ and $a = 0.05$. The error correction gains $K_k^{\mathcal{C}}$ for the curve position and K_k^{β} for the curve's normal velocity were both 0.25. Initial conditions (the bold solid curves) were chosen far from the initial measurement curves (dash-dotted curves). For the single blob case, the estimated curve (solid curve) converges nicely to the measurement curve over time. For the two blobs case, the estimated curve undergoes topological changes; the curves merge and split naturally.

IX. CONCLUSIONS AND FUTURE WORKS

A. Conclusions

This paper proposed geometric observers for dynamically evolving curves that can be implemented completely implicitly (using transport equations). In comparison to most previous approaches there is no finite dimensional motion model, allowing for the natural handling of topological changes. Due

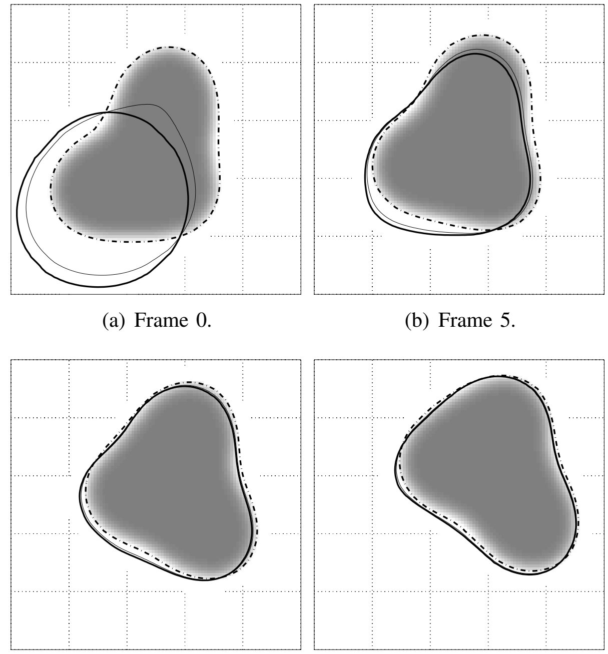

(a) Frame 0. (b) Frame 5. (c) Frame 10. (d) Frame 15.

Fig. 5. Tracking of a single blob. The bold solid line is the prediction, the dash-dotted line the measurement, and the solid line the interpolated curve. Error correction gains for position and normal velocity are both 0.25.

to the geometric nature of the proposed observer, observer gains become geometrically meaningful.

State measurements are performed via static segmentations, making the framework flexible and powerful, since any kind of curve segmentation may be used for the measurement step, including curve segmentations incorporating shape information. In this way, measurements can induce shape information to the estimated curve without the need for explicit incorporation of shape information into the motion prior.

B. Future Works

The motion priors proposed in this paper are simple. While accurate motion models may be out of reach for many applications, investigating different motion priors (e.g., motion priors that are area-preserving, length-preserving, smoothness-limiting, etc.) may be fruitful.

The main drawback of the currently proposed observer scheme is that it makes no use of statistical information, i.e., a "measure-of-trust" for measurements and the observed states. Introducing statistical information will require the notion of a mean shape of curves and curve covariances [13]. Future work will introduce adaptive observer gains based on curve statistics.

An exciting research topic is the inclusion of (dynamically changing) shape information into the measurement step. Shape information may also be incorporated into the "measure-of-trust", by comparing measurements with and without shape information. In cluttered environments or in case of occlusions and poor image information using shape

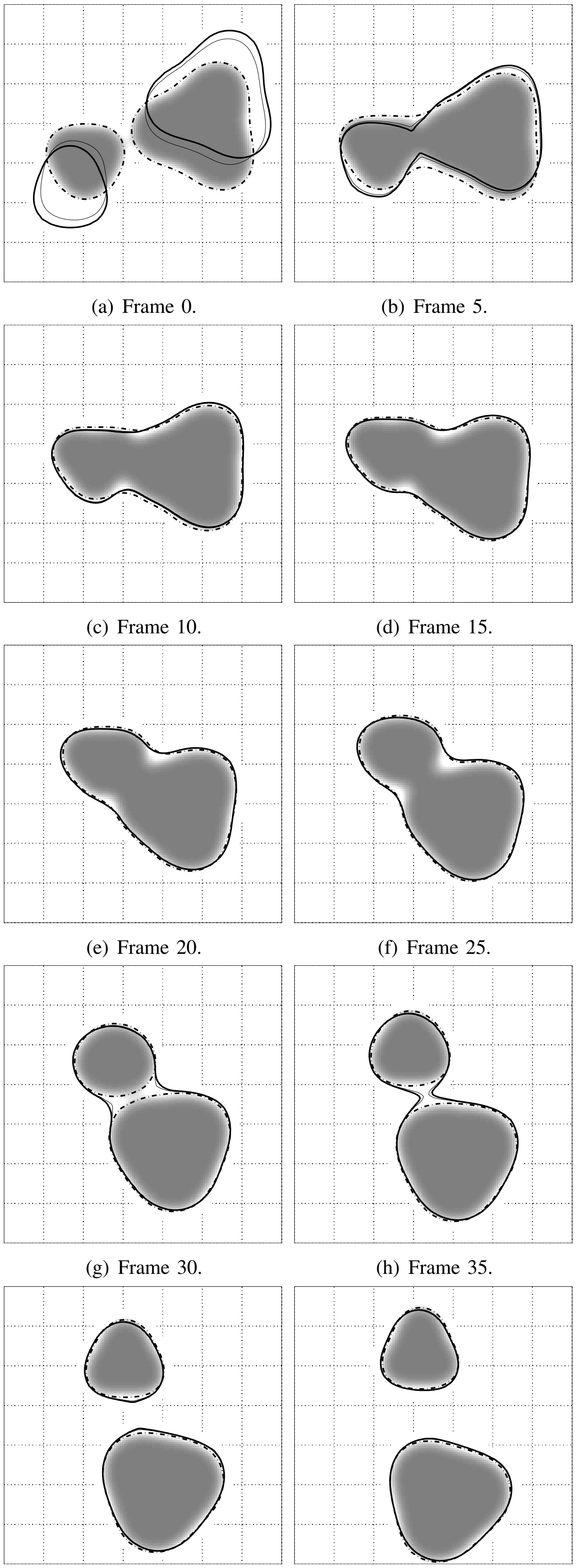

(a) Frame 0. (b) Frame 5.

(c) Frame 10. (d) Frame 15.

(e) Frame 20. (f) Frame 25.

(g) Frame 30. (h) Frame 35.

(i) Frame 40. (j) Frame 45.

Fig. 6. Tracking of a two blobs. The bold solid line is the prediction, the dash-dotted line the measurement, and the solid line the interpolated curve. Error correction gains for position and normal velocity are both 0.25.

information is crucial to improving tracking robustness. Should there be a complete loss of tracking, graceful degradation needs to be ensured. Further, tracking performance on real image sequences needs to be explored.

Some of these issues will be addressed in [14].

REFERENCES

[1] A. Yezzi and S. Soatto, "Deformotion: Deforming motion, shape average and the joint registration and approximation of structures in images," *International Journal of Computer Vision*, vol. 53, no. 2, pp. 153–167, 2003.

[2] J. D. Jackson, A. J. Yezzi, and S. Soatto, "Tracking deformable moving objects under severe occlusions," in *Proceedings of the Conference on Decision and Control*. IEEE, 2004.

[3] S. Osher and R. Fedkiw, *Level Set Methods and Dynamic Implicit Surfaces*, ser. Applied Mathematical Sciences. Springer-Verlag, 2003, vol. 153.

[4] M. Niethammer, A. Tannenbaum, and S. Angenent, "Dynamic geodesic snakes for visual tracking," submitted to the *IEEE Transactions on Automatic Control*, 2004.

[5] D. Cremers and S. Soatto, "A pseudo-distance for shape priors in level set segmentation," in *Proceedings of the International Workshop on Variational, Geometric and Level Set Methods in Computer Vision*. IEEE, 2003, pp. 169–176.

[6] A. Blake and M. Isard, *Active Contours*. Springer Verlag, 1998.

[7] T. F. Chan and L. A. Vese, "Active contours without edges," *IEEE Transactions on Image Processing*, vol. 10, no. 2, pp. 266–277, 2001.

[8] E. Pichon, M. Niethammer, and D. Nain, "A Laplace equation approach for the validation of image segmentation," in preparation.

[9] A. Duci, A. J. Yezzi, S. K. Mitter, and S. Soatto, "Shape representation via harmonic embedding," in *Proceedings of the International Conference on Computer Vision*, 2003, pp. 656–662.

[10] A. Yezzi and J. L. Prince, "A PDE approach for measuring tissue thickness," in *CVPR*, vol. 1, 2001, pp. 87–92.

[11] R. J. Leveque, *Finite Volume Methods for Hyperbolic Problems*. Cambridge Texts in Applied Mathematics, 2002.

[12] C. Y. Kao, S. Osher, and Y.-H. Tsai, "Fast sweeping methods for static Hamilton-Jacobi equations," UCLA, Tech. Rep. 03-75, 2003.

[13] G. Charpiat, O. Faugeras, and R. Keriven, "Approximations of shape metrics and application to shape warping and empirical shape statistics," *Foundations of Computational Mathematics*, pp. OF1–OF58, 2004.

[14] M. Niethammer, P. A. Vela, and A. Tannenbaum, "Geometric observers for dynamically evolving curves," in preparation.